

# AgenticLab: A Real-World Robot Agent Platform that Can See, Think, and Act

Pengyuan Guo<sup>1,\*</sup>, Zhonghao Mai<sup>1,\*</sup>, Zhengtong Xu<sup>1,\*</sup>, Kaidi Zhang<sup>1</sup>, Heng Zhang<sup>2</sup>, Zichen Miao<sup>1</sup>, Arash Ajoudani<sup>2</sup>, Zachary Kingston<sup>1</sup>, Qiang Qiu<sup>1</sup>, Yu She<sup>1</sup>

<sup>1</sup>Purdue University

<sup>2</sup>Istituto Italiano di Tecnologia

\*Equal contribution.

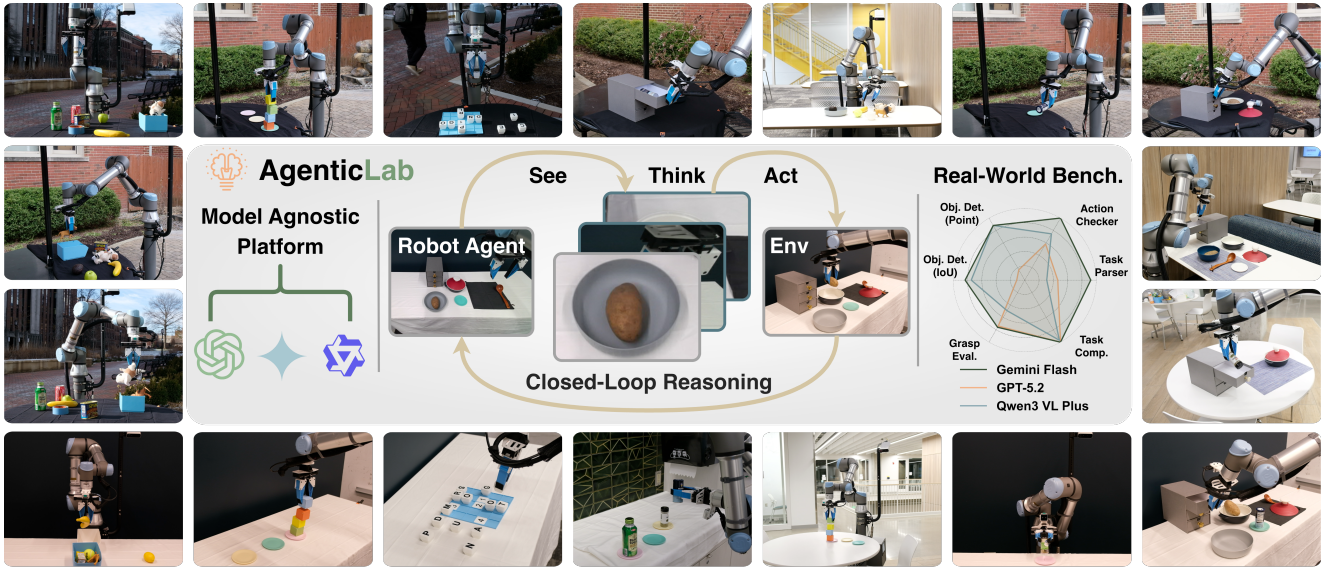


Fig. 1: AgenticLab is a model-agnostic real-world robot agent platform that uses onboard cameras and open-vocabulary language prompts to manipulate in unstructured environments, with closed-loop reasoning that interleaves execution, verification, and replanning throughout manipulation.

**Abstract**—Recent advances in large vision-language models (VLMs) have demonstrated generalizable open-vocabulary perception and reasoning, yet their real-robot manipulation capability remains unclear for long-horizon, closed-loop execution in unstructured, in-the-wild environments. Prior VLM-based manipulation pipelines are difficult to compare across different research groups’ setups, and many evaluations rely on simulation, privileged state, or specially designed setups. We present AgenticLab, a model-agnostic robot agent platform and benchmark for open-world manipulation. AgenticLab provides a closed-loop agent pipeline for perception, task decomposition, online verification, and replanning. Using AgenticLab, we benchmark state-of-the-art VLM-based agents on real-robot tasks in unstructured environments. Our benchmark reveals several failure modes that offline vision-language tests (e.g., VQA and static image understanding) fail to capture, including breakdowns in multi-step grounding consistency, object grounding under occlusion and scene changes, and insufficient spatial reasoning for reliable manipulation. We will release the full hardware and software stack to support reproducible evaluation and accelerate research on general-purpose robot agents.

## I. INTRODUCTION

Recent progress in large vision-language models (VLMs) has enabled strong open-vocabulary visual understanding and language-conditioned reasoning [1, 5, 31]. An open question

is how reliably these generalist models support real-robot manipulation, where success depends on closed-loop coupling between perception, decision-making, and execution over long horizons [14, 28, 5].

Recent evaluations of VLMs in embodied settings remain difficult to interpret for real robots. Many benchmarks use question-answering or offline interfaces that approximate embodied reasoning without executing actions [28, 27]. Moreover, simulation-based evaluations cannot fully capture real-world dynamics, partial observability, and actuation/perception noise [32]. As a result, these evaluations often miss failure modes that only emerge under closed-loop reasoning with execution, where the agent must repeatedly perceive, act, verify outcomes, and replan.

Real-robot VLM systems partially address this gap but still complicate standardized benchmarking. Many are evaluated in constrained scenes with limited object states or categories [34, 35], which under-represent long-horizon errors such as complex lighting conditions, disturbances (e.g., wind), background change, and occlusion. Others rely on one-shot planning that lacks feedback-driven correction and replanning during execution [33, 12]. Finally, although some works ablate

specific components, many systems are validated on a single (or few) VLMs and include model-specific designs [13, 30]. This makes it hard to compare different model families under a consistent execution protocol.

In parallel, vision-language-action models (VLAs) attempt to unify perception, reasoning, and control into holistic architectures [16, 14]. Although promising, their zero-shot manipulation performance is often limited, and strong results typically rely on fine-tuning with substantial task-specific robot demonstrations [14]. More critically, fine-tuning often creates a trade-off: as the model specializes in specific motor skills, it frequently suffers from catastrophic forgetting, diminishing the open-world generalization capabilities inherent in the pretrained backbone [9, 36]. This limits their adaptability in unstructured environments where conditions shift unpredictably.

In this paper, we present **AgenticLab**, a model-agnostic real-world robot agent platform. The contributions of this work are threefold:

1. We introduce a robot agent pipeline for open-world, open-vocabulary manipulation with vision-language closed-loop reasoning. Unlike prior systems that rely on open-loop planning or privileged state, our agent perceives unstructured scenes, decomposes tasks, executes actions, and iteratively verifies and replans from visual feedback. The pipeline is model-agnostic, allowing different VLMs (e.g., Gemini [5], GPT [1], Qwen [31]) to be swapped in through a unified interface, enabling fair evaluation without model-specific engineering.

2. We present a real-world benchmark to evaluate the embodied performance of modern VLMs. Unlike prior VLM benchmarks that focus on static image understanding and open-loop VQA, and manipulation benchmarks that are largely simulation-based, our suite evaluates grounded perception, spatial reasoning, and sequential decision-making under closed-loop execution on physical robots. We assess models via both module benchmarks and end-to-end rollouts, revealing large real-world performance gaps and failure modes that VQA, static image understanding, and simulation benchmarks often miss.

3. We release an open-source platform design that enables direct deployment of VLM-based agents for in-the-wild robot manipulation. The platform integrates sensing, control, and agentic reasoning into a system that is easy to assemble and reproduce, lowering the barrier to entry for embodied intelligence research and empowering the community to rapidly iterate on new algorithms and tackle the practical challenges of running large foundation models on physical hardware.

## II. RELATED WORK

### A. VLM-based Robot Manipulation

A common paradigm for VLM-based manipulation is to query a VLM with images and language instructions to produce a plan, program, or a small set of subgoals that are then executed by a separate perception–planning–control stack. Many such systems remain largely open-loop: they generate a static plan and execute it with limited state verification, making

them brittle to grasp failures, object movement, slippage, and scene changes [12, 33, 3, 20].

Current VLM-based manipulation is still often benchmarked in controlled settings with curated layouts and limited appearance variation [34, 35, 6, 29]. In the wild, changes in lighting, disturbances, and background shifts can quickly invalidate the initial grounding, causing small errors to compound over long-horizon execution.

Another challenge is comparability across models and systems. Prior frameworks often incorporate model-specific prompts, tools, or design choices and are typically demonstrated with only one or a few VLMs [13, 30, 21, 8, 26]. As a result, it is difficult to disentangle model capability from system-level engineering and to compare different VLM families under the same sensing-to-action protocol. Some works provide component-level comparisons [21], but unified, drop-in evaluation across diverse VLMs remains limited.

AgenticLab addresses these challenges with a model-agnostic, real-world robot agent platform for open-world manipulation. It executes a closed-loop pipeline that interleaves task parsing, grounding, planning, execution, and verification, and triggers replanning for failure recovery during long-horizon rollouts.

### B. Embodied Benchmarks for VLMs

Many embodied benchmarks for VLM adopt QA-style or offline interfaces to probe visual reasoning and spatial language understanding without executing actions in the world [28, 27, 24, 2]. While valuable for controlled diagnosis, the central limitation is the absence of action execution: without embodied interaction, these settings cannot test whether a model can sustain grounding under action-induced scene changes, detect and correct failures online, or remain robust to error accumulation over long horizons.

Simulation-based benchmarks add interactivity and scale by standardizing environments and task suites [32, 18, 15, 22, 4, 23]. However, these simulators necessarily simplify the world and the action interface: scenes often use cleaner layouts and idealized object states, and actions can be executed through abstracted primitives without requiring full physical realism. As a result, success in simulation may overestimate robustness and may not translate to reliable physical execution.

AgenticLab provides a reproducible, open-source hardware and software stack and supports a real-robot benchmark for evaluating VLMs as closed-loop agents through repeated perception, verification, and recovery. It exposes failures caused by clutter and occlusion, complex lighting, object movement, and scene changes that offline tests and simulation often miss.

## III. REPRODUCIBLE PLATFORM FOR ROBOT AGENT DEPLOYMENT

Our platform prioritizes reproducibility, robustness, and real-world deployability. We adopt a general-purpose hardware design that transfers across environments, rather than being tailored to a task-specific setup. Fig. 2 provides an overview of the system.

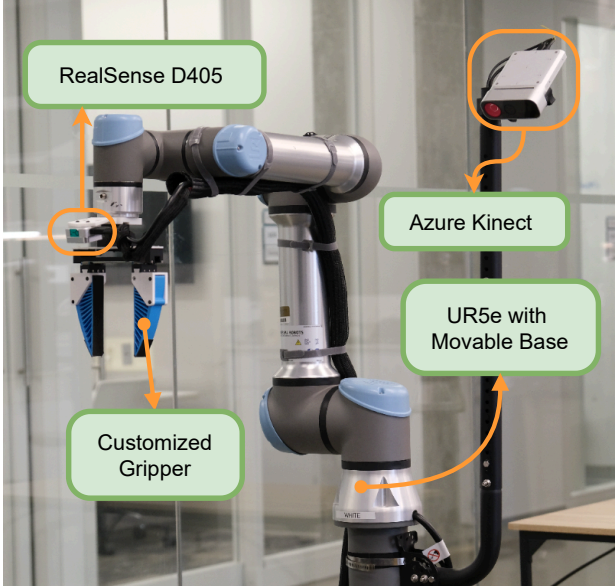


Fig. 2: The AgenticLab Manipulation Platform: a fully reproducible, easy-to-deploy platform for real-world, in-the-wild robot agent benchmark.

We use two RGB-D views to combine global scene context with close-range feedback. An Azure Kinect provides a fixed shoulder view for scene grounding and layout understanding, while a wrist-mounted RealSense D405 captures detailed observations for local close-range feedback. We chose this pair because they offer complementary effective depth ranges and compact form factors. A UR5e arm is mounted on a movable base for deployment across indoor and outdoor scenes.

We build a low-cost parallel gripper with fin-ray fingers driven by a single servo. The gripper uses 3D-printed parts and off-the-shelf components, costs under \$200, and provides repeatable actuation for grasping a diverse set of everyday objects.

To support reliable deployment and reproducible evaluation, we implement a lightweight robotics stack with core utilities for trajectory generation, inverse kinematics, and multi-camera calibration. Using calibrated depth, we lift 2D image coordinates to metric 3D points in the robot base frame, enabling consistent spatial grounding across environments.

#### IV. MODULAR CLOSED-LOOP ROBOT AGENT FRAMEWORK

In this section, we describe the system design of AgenticLab, a closed-loop robot agent framework that executes actions, monitors outcomes, and revises plans as needed during in-the-wild manipulation. As illustrated in Fig. 3, our system design is guided by three core principles that structure the robot agent framework:

**1. Model-Agnostic Pipeline:** AgenticLab is designed around a unified interaction interface that allows drop-in replacement of the VLM, enabling different models to be evaluated under the same pipeline and protocol.

**2. Closed-Loop Reasoning:** AgenticLab iteratively uses visual feedback to verify action preconditions and effects, detect failures and uncertainty, and trigger replanning for long-horizon, in-the-wild manipulation.

**3. Module Design and Functional Decomposition:** The pipeline is decomposed into modules with clear responsibilities, making components interpretable, compositional, and swappable. This enables controlled, module-level benchmarking of VLM capabilities in grounding, understanding, and reasoning, while allowing easy integration of external tools.

##### A. See: Multi-View Open-Vocabulary Perception

AgenticLab converts RGB-D observations into structured scene representations to support open-vocabulary grounding and spatial reasoning. This process provides the essential object information and geometric relations required for downstream planning and execution.

Grounding is implemented via a unified interface that supports swappable perception strategies. For instance, the system can rely on a VLM to directly predict object locations, or employ LangSAM [25] for segmentation with subsequent VLM verification for object correctness. This modular design supports open-vocabulary detection and enables models without native grounding capabilities to operate effectively via external tools.

Perception operates iteratively, initializing the scene representation at the start and providing visual feedback after each action. Importantly, AgenticLab does not assume perfect perception. Through closed-loop feedback, the agent can adapt to visual noise, such as variable lighting and background changes, that would otherwise degrade single-shot perception systems.

As an example of fine-grained interaction, the agent leverages a wrist-mounted camera to refine grasp results. The VLM decides when to switch from the global shoulder view to the local wrist view based on verification feedback. For example, if a candidate grasp is rejected due to collision risks, the system acquires a local wrist view of the target region to replan the grasp pose, as shown in Fig. 3. Additional closed-loop perception behaviors, including reflective visual grounding and scene understanding, are described in the appendix.

##### B. Think: Model-Agnostic Reasoning and Planning

AgenticLab adopts a model-agnostic, closed-loop interaction paradigm that mediates all communication between VLMs and the execution stack. It enforces a consistent protocol for querying any VLM and translating its output for task parsing, planning, and verification. As shown in Fig. 3, the agent's reasoning is organized into several interacting modules.

**1. Task Parser:** To bridge unstructured language and executable logic, the task parser converts the instruction into a structured Planning Domain Definition Language (PDDL) problem, following the LLM-guided symbolic planning paradigm [19, 34]. With a predefined PDDL domain file specifying action parameters, preconditions, and effects, the VLM instantiates a task-specific problem file by grounding

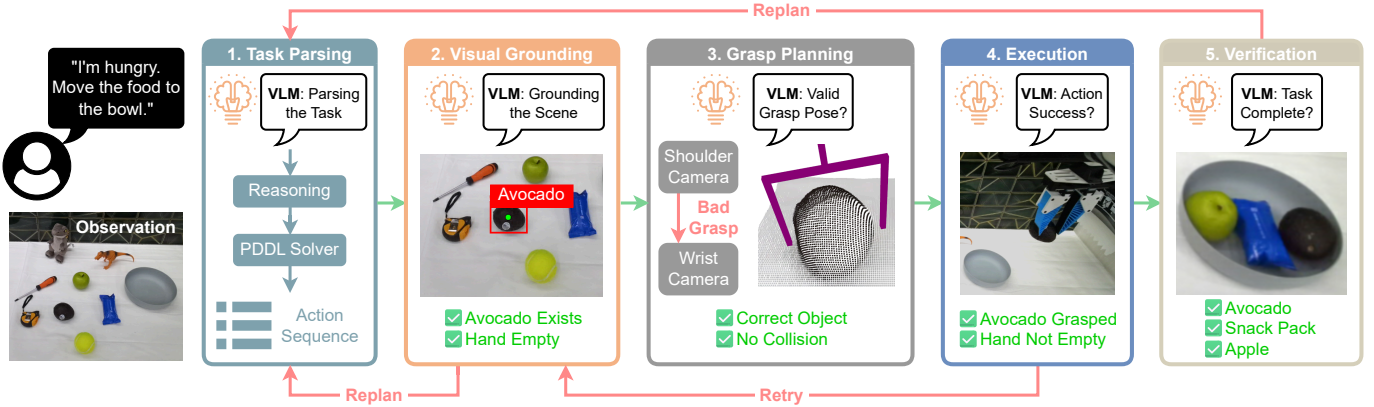


Fig. 3: Pipeline of AgentLab. AgentLab executes a closed-loop agentic reasoning pipeline for manipulation that integrates task parsing, grounding, planning, execution, verification, and replanning. As illustrated in the figure, a human provides a natural-language instruction, and the robot first acquires onboard observations and parses the task to produce an initial plan. The agent then follows the green arrows to execute each block in sequence, carrying out each step of the initial plan along this path until all planned steps are completed. Each block includes a VLM-based verification step: if verification succeeds, execution proceeds to the next block along the green path; otherwise, the agent follows the red arrows to retry or replan based on updated observations. For grasp planning, the agent first plans grasps using the shoulder camera; if grasp verification fails, it replans with the wrist camera for more localized visual cues.

objects, initial-state predicates, and goal predicates from visual observations and language instructions. A symbolic planner based on Fast Downward [10] then generates a sequence of high-level action primitives that satisfy the specified goals. By explicitly representing action preconditions and effects in the PDDL domain file, symbolic planning enables stable long-horizon execution and circumvents the unpredictability associated with unconstrained free-form text generation.

**2. Action Checker:** Before each action, the action checker evaluates whether the required preconditions hold and whether the action is feasible in the current scene. After execution, the system re-observes the environment and reassesses action effects using updated visual input. Upon completion of all planned actions, the action checker further verifies whether the final scene satisfies all the goal conditions. These verification steps detect failures such as missed grasps, incorrect object interactions, or unexpected state changes.

**3. Grasp Planner:** Candidate grasp poses are first generated from RGB-D observations using AnyGrasp [7]. The best candidate is then evaluated by a VLM to determine semantic correctness and physical feasibility, specifically whether the grasp targets the intended object and whether it is likely to cause collision or instability. As shown in Fig. 3, the agent first plans grasps from the shoulder camera; if a candidate is rejected, it replans using the wrist camera to obtain more localized visual evidence and refine grasp selection.

#### C. Act: Primitive-Based Execution

AgentLab abstracts robot behavior into a set of high-level action primitives, including pick, place, and open/close drawer. Each primitive represents a semantically meaningful action that can be composed to solve multi-step tasks.

Action primitives are executed using position-based control. For the pick primitive, the VLM specifies a grasp region of interest via visual grounding, and AnyGrasp generates candidate 6-DoF grasp poses and gripper width within this region. The robot then performs Cartesian-space trajectory generation by constructing a sequence of intermediate waypoints to reach the selected grasp pose and execute the grasp.

Execution is monitored through discrete outcome verification after each action. Failure cases include unsuccessful grasps and actions that leave the scene unchanged. These signals are propagated to the reasoning module, enabling closed-loop behaviors such as retrying the action or replanning based on updated observations.

## V. EXPERIMENT SETUP

### A. Benchmark Design Principles

Our benchmark is designed to expose embodied agent capabilities that are not well captured by simulation benchmarks, static image understanding, and VQA-style evaluations. We curate a diverse set of tasks that expose the dominant failure modes relevant to physical deployment of VLMs. Three principles guide our benchmark design:

1. We require open-vocabulary grounding: instructions include ambiguous references, attributes, and spatial relations, so models must maintain object identity and consistent grounding across multiple steps.

2. We emphasize long-horizon, error-amplifying execution, where perception, verification, and replanning are invoked repeatedly; robust performance requires online failure detection and recovery.

3. We evaluate our system’s generalization on five representative tasks across three settings: controlled lab scenes, realistic

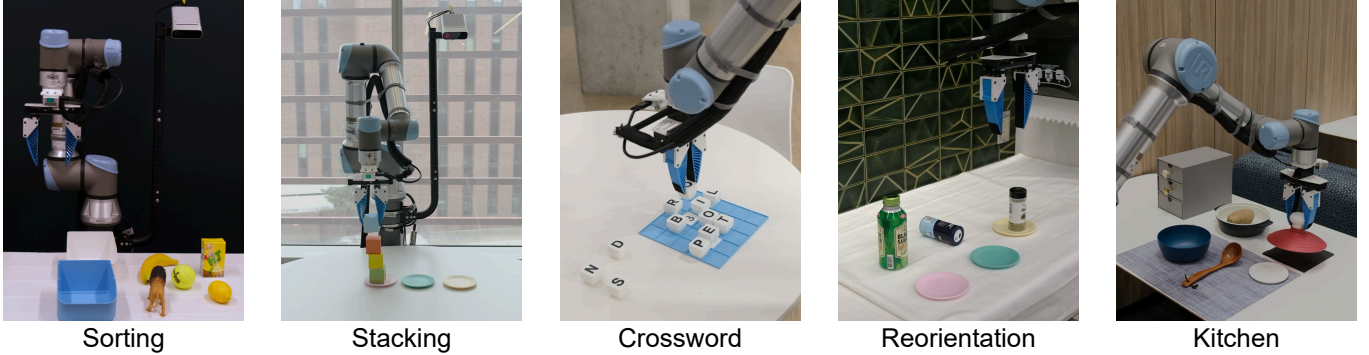


Fig. 4: Manipulation tasks used for real-world evaluation and benchmark. These tasks are selected to cover a range of challenges, including spatial reasoning, vision-language grounding, and long-horizon planning.

indoor kitchens, and unstructured outdoor environments. These diverse conditions explicitly test robustness against variations in lighting, clutter, occlusion, and background shift.

#### B. Tasks and Scenes

We design a suite of five real-world robot manipulation tasks to evaluate embodied vision-language reasoning under challenging conditions. Together, these tasks span grounded object understanding, spatial reasoning, and long-horizon sequential planning, making them well-suited for assessing closed-loop agent behavior.

The task suite is shown in Fig. 4. **Sorting** categorizes 3-7 objects into designated bins based on semantic or visual attributes, stressing compositional grounding and ambiguity resolution. **Stacking** vertically arranges objects in the exact order specified in the prompt, requiring instruction-following vision-language reasoning, precise placement, and stability under strong sequential dependencies. **Crossword** arranges letter blocks to form up to three intersecting words on a grid, combining world knowledge with fine-grained placement. **Reorientation** adjusts an object’s pose to satisfy language-specified orientation constraints, emphasizing spatial understanding beyond 2D placement. **Kitchen** is a long-horizon rearrangement task that places items into context-appropriate containers or regions, stressing sustained grounding and recovery.

We evaluate all tasks across three scene settings: controlled laboratory setups, cluttered indoor kitchens, and unstructured in-the-wild outdoor environments.

## VI. EXPERIMENTAL RESULTS AND ANALYSIS

In our experimental evaluation, we seek to investigate the following five key questions regarding the viability of VLMs as embodied agents:

1. Can a single VLM reliably operate an end-to-end, closed-loop robot agent (Section VI-A)?
2. Which modules are the primary bottlenecks for real-world execution (Section VI-B)?
3. Does a compositional pipeline generalize better than a single VLM (Section VI-C)?
4. What is the impact of ablating the action checker and the grasp planner (Section VI-D)?

TABLE I: Performance of single-VLM pipelines on the sorting task. Each pipeline uses one VLM for all modules and is evaluated over 20 trials across 6 object setups.

Model Pipeline	Success Rate	Time	Tokens
Gemini 3 Flash	<b>75.0 %</b>	334 s	67.0k
Gemini 3 Pro	10.0 %	1283 s	139.0k
Gemini 3 Pro + LangSAM	70.0 %	524 s	80.9k
Gemini Robotics	50.0 %	382 s	<b>40.6k</b>
Qwen-VL-Max	0.0 %	–	–
Qwen3-VL-Plus	25.0 %	538 s	43.0k
GPT-5.2 + LangSAM	0.0 %	–	–
GPT-4o + LangSAM	5.0 %	<b>299 s</b>	49.6k

5. How does AgentLab compare to fine-tuned VLAs (Section VI-E)?

#### A. Can a Single VLM Drive a Robot Agent?

We first test whether a single VLM can operate the complete AgentLab pipeline. We evaluate eight models on the sorting task over 20 trials across six object setups spanning fruits, blocks, toys, and tools, and report success rate, runtime, and token usage in Table I, with dominant failure modes summarized in Fig. 5.

The Gemini family is the most consistent. Gemini Flash achieves the highest success rate at 75.0% with low latency, balancing fast reasoning with accurate visual grounding. Gemini Pro is strong in abstract reasoning but less reliable in visual grounding. As shown in Table I, Gemini Pro exhibits unstable object detection that triggers repeated re-queries and overthinking; performance improves when replacing the detector with LangSAM.

Models such as Qwen-VL-Max and GPT-5.2 achieve near-zero success primarily due to unreliable execution-state verification. A common failure mode is hallucination during action checking. For example, the model may claim the object is not in the gripper after a successful pick.

This experiment shows that an embodied agent’s robustness is bounded by its weakest repeatedly invoked capability, and that verification quality can dominate end-to-end performance in ways that VQA and static-image benchmarks fail to capture. For example, in our sorting task, placing three objects triggers

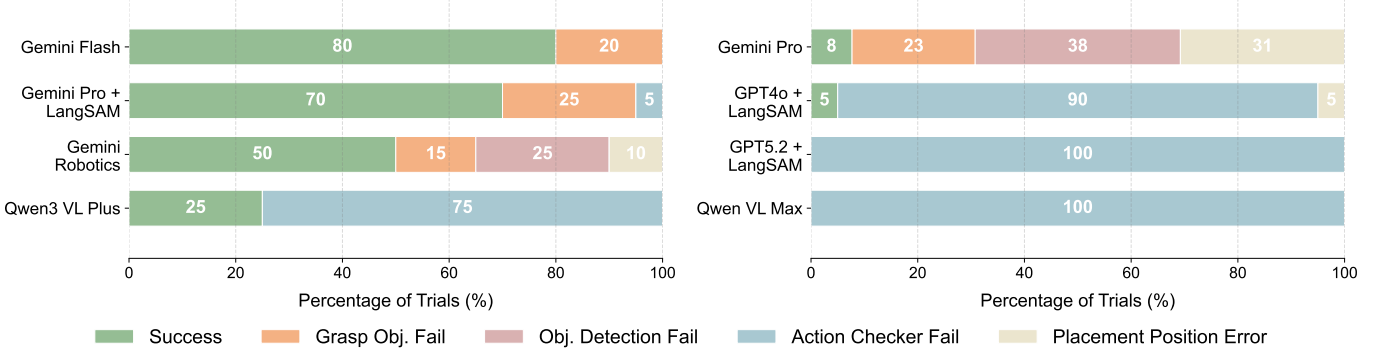


Fig. 5: Failure mode breakdown for single-VLM pipelines on the sorting task. Results show which pipeline components dominate failures across different VLMs.

six calls to the action checker. As a result, even with 90% accuracy on static action-predicate VQA, the probability of completing a full trial is only  $0.9^6 \approx 0.53$ . More critically, at 50% accuracy, success collapses to  $0.5^6 \approx 1.5\%$ . This compounding effect explains why models with seemingly moderate verification errors in isolation can fail catastrophically under closed-loop execution.

#### B. Module Benchmark

To attribute end-to-end outcomes to concrete sources, we isolate and evaluate five modules within the closed-loop agetic pipeline: task parser, object detector, action checker, grasp planner, and goal checker, as summarized in Table II. Each module is tested across multiple scenes and tasks for different models, using consistent prompts and the same sensory stack. Experimental details are provided in the appendix.

As shown in Table II, Gemini Flash and Pro achieve high task-parser success across diverse tasks. Locally deployed models, such as Qwen2.5-VL-7B and Molmo-7B, perform substantially worse. They often struggle with long-context, structured plan generation. Common failure modes include corrupted PDDL syntax and missing constraints. Overall, these results suggest that language-to-symbolic translation is not the primary bottleneck for current cloud-hosted models.

For the object detector, model size does not correlate with performance. Specialized or local models such as Qwen3-VL-Plus and Molmo-7B demonstrate pointing accuracy competitive with or superior to larger models such as Claude-4.5-Sonnet. This suggests that visual grounding is a distinct capability that can be effectively offloaded to smaller, specialized architectures. Qwen models show strong pointing performance at 81-88% but high variance in bounding-box correctness, remaining accurate when grounding succeeds yet prone to complete misidentification in cluttered scenes.

Confirming the insight from Section VI-A, while most models achieve more than 50% success in isolated VQA-style action checker tests, this is insufficient for deployment. The same models fail almost immediately in full-pipeline execution because verification errors compound under real-world distribution shift.

Action verification demands a higher level of semantic understanding than static scene grounding. While grounding relies primarily on detection and spatial reasoning, verification requires interpreting complex interaction semantics: for example, discerning whether an object is securely grasped despite the visual occlusion caused by the gripper.

Grasp evaluator performance correlates with the capability of thinking rather than visual grounding. Gemini Pro at 77.8%, GPT-5.2 at 75.9%, and Claude Opus at 70.4% perform best because they can reason about interaction-level semantics, including collision risk, grasp stability, and target-object mismatches. Detailed metrics are provided in the appendix.

We report runtime as an averaged estimate from randomized evaluations conducted across multiple time periods. While latency for cloud-hosted models is largely determined by the provider’s service, our goal is to provide an intuitive sense of query-time differences across models, enabling practitioners to make informed deployment choices for robotic agents based on their efficiency requirements.

#### C. Compositional Pipeline vs. Single VLM

Guided by the module benchmark in Section VI-B, we construct a compositional pipeline that assigns failure-sensitive modules to specialist models: Gemini Flash handles task parsing and grasp planner, Qwen3-VL-Plus performs visual grounding, and Claude Opus assesses task completion. We compare this pipeline against a single-VLM Gemini Flash baseline across lab, kitchen, and outdoor settings, with results reported in Fig. 6.

For this experiment, we report a task progress score computed from a structured rubric (see appendix). This metric captures partial completion and is more informative than binary success.

We disable action-level verification and retain only task-level completion checks. This reduces rollout latency and supports longer-horizon execution. It also enables a cleaner evaluation of closed-loop reasoning, planning, and visual grounding under lighting changes, clutter, and occlusion. We analyze the cost-benefit of dense action verification separately in the ablation study in Section VI-D.

TABLE II: Module benchmark of VLMs for AgenticLab. SR denotes success rate; “–” indicates the VLM cannot generate usable results for the module.

Model	Task Parser		Action Checker		Object Detector			Grasp Planner		Goal Checker		
	SR (%)	Time	SR (%)	Time	Pointing SR (%)	Bbox IoU (%)	Time	SR (%)	Time	SR (%)	Time	
Gemini	Gemini 3 Pro	<b>92.3</b>	70.5	98.4	13.3	66.7	53.7	45.7	<b>77.8</b>	26.8	<b>100.0</b>	8.4
	Gemini 3 Flash	<b>92.3</b>	45.2	<b>100.0</b>	<b>5.3</b>	<b>88.1</b>	<b>83.4</b>	9.5	74.1	9.1	<b>100.0</b>	15.6
	Gemini Robotics	75.0	29.6	95.1	10.1	57.1	40.4	5.8	55.0	10.3	<b>100.0</b>	13.5
Qwen	Qwen3-VL-Plus	30.8	40.2	74.6	11.4	<b>88.1</b>	74.8	5.1	66.7	10.0	96.9	12.1
	Qwen-VL-Max	17.3	36.3	64.8	24.2	81.0	60.3	5.0	59.2	9.7	84.4	11.2
Others	GPT-5.2	46.2	31.8	58.2	8.6	16.6	11.2	<b>3.2</b>	75.9	8.0	<b>100.0</b>	9.1
	GPT-4o	48.1	<b>16.0</b>	68.9	7.0	14.3	8.0	3.9	44.4	<b>4.4</b>	93.8	<b>5.1</b>
	Claude-4.5-Opus	78.9	17.0	64.8	7.1	9.6	6.1	4.4	70.4	8.2	93.8	6.6
	Claude-4.5-Sonnet	40.4	17.2	40.4	11.9	61.9	43.9	4.1	54.7	9.6	78.1	10.0
Local	Qwen2.5-VL-7B	–	–	25.8	8.1	73.8	51.0	6.6	–	–	50.0	9.2
	Molmo-7B	–	–	33.9	19.0	76.2	27.0	3.6	–	–	43.8	18.1

As shown in Fig. 6, the compositional pipeline does not consistently outperform the Gemini Flash baseline. Both pipelines exhibit a robustness gap when transitioning from controlled lab trials to shifted environments, with the largest drops in tasks that require fine placement and sustained identity tracking.

Composition is most effective when errors are attributable to a single bottleneck module. For stacking, replacing the grounding component with Qwen3-VL-Plus improves localization and stabilizes precision-critical placement. For reorientation, we instead use Gemini Pro only for this task to better handle pose-conditioned reasoning and orientation constraints, isolating the benefit of stronger 3D semantic understanding without changing the rest of the pipeline.

Overall, these results demonstrate the inherent advantage of the compositional pipeline: the flexibility to compensate for the limitations of a single VLM through strategic model selection. Crucially, this paradigm offers a practical pathway to improve system performance without the prohibitive computational cost of end-to-end retraining, enabling efficient system optimization.

#### D. Ablation Study: Action Checker and Grasp Planner

In this experiment, we characterize the robustness–efficiency trade-off via targeted ablations of two components. First, we compare three action-checking configurations: no checker, goal checker only, and full action checker, under controlled disturbances (Fig. 7). Second, we ablate the grasp planner by enabling or disabling grasp evaluation, as shown in Fig. 8(a).

We run the action checker ablations on two tasks: sorting, where actions are weakly coupled, and sequential stacking, where actions are strongly dependent and early failures affect all subsequent actions. For the grasp planner, we ablate grasp evaluation on sorting in clustered scenes, where imperfect bounding boxes often include multiple objects and collision-prone grasps are common.

Two patterns emerge. First, grasp evaluation is critical in cluttered scenes. When it is disabled, task success drops sharply because the system is more likely to execute collision-



Fig. 6: Performance comparison across environments. We compare a Gemini Flash baseline with a compositional pipeline across five manipulation tasks. Performance is measured using a task progress score that quantifies partial completion.

prone grasps or pick the wrong object when the detected workspace contains multiple nearby items.

Second, verification frequency determines when errors are detected. Although a full action checker increases execution time, it can correct mistakes by detecting failures early. In stacking, disabling verification leads to zero task success because early errors propagate and the final stack violates the target order. Using only a goal checker delays error detection until task completion: the system continues stacking despite previous mistakes, producing an invalid intermediate stack and requiring replanning from a more complex state, which results in unnecessary actions and increased execution time. Full action checker instead enables early detection and timely recovery.

Overall, these results point to a practical guideline: sparse verification improves evaluation efficiency, whereas dense verification is required when tasks involve strong dependencies or active disturbances.

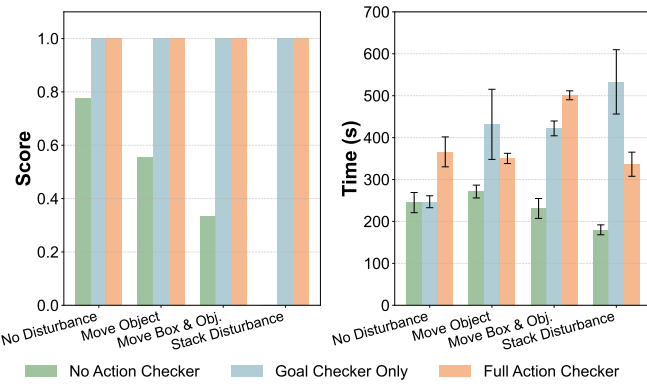


Fig. 7: Action checker ablation across disturbance scenarios. We report task progress score and execution time for three verification modes: no action checker, goal checker only, and full action checker. Error bars denote standard deviation.

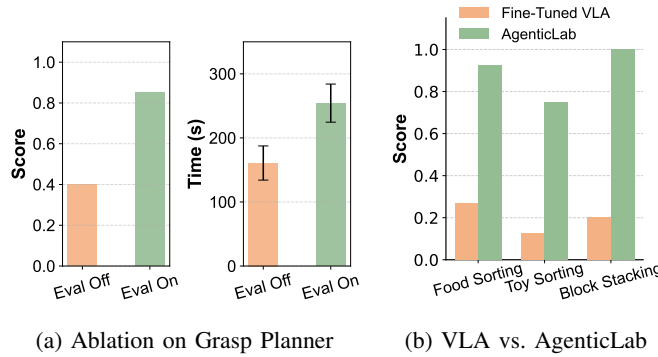


Fig. 8: (a) Ablation study on the grasp planner. We compare performance and execution time with grasp evaluation enabled and disabled. Enabling grasp evaluation improves performance in cluttered scenes, at the cost of increased execution time. (b) Performance comparison between a fine-tuned VLA and AgenticLab. We compare a  $\pi_{0.5}$  VLA fine-tuned with 40 demonstrations for sorting and 30 demonstrations for stacking against the AgenticLab pipeline on both tasks.

#### E. Off-the-Shelf VLA vs. AgenticLab

Finally, we compare AgenticLab against the state-of-the-art VLA  $\pi_{0.5}$  [14]. We fine-tune  $\pi_{0.5}$  using 40 demonstrations for sorting and 30 demonstrations for stacking. We keep prompts, task definitions, and evaluation metrics aligned to our benchmark and follow the same protocol as Sec. VI-C. Training time and data collection details are provided in the appendix.

As shown in Fig. 8(b), the VLA baseline underperforms the AgenticLab pipeline. Fine-tuned VLAs struggle to satisfy fine-grained semantic constraints in natural-language instructions. For example, in sorting tasks, when instructed to grasp a toy, the fine-tuned VLA may instead pick up a food item, indicating unreliable instruction grounding. Moreover, the VLA baseline often fails to achieve precise grasp poses or

accurate placement. These behaviors reflect a key limitation of VLAs: while they can represent effective motor primitives, they do not reliably acquire task decomposition, high-level reasoning, and closed-loop verification and recovery. These capabilities are essential for open-world manipulation under actuation and perception uncertainty. By decoupling reasoning, grounding, and execution and integrating them into a closed-loop agentic pipeline, AgenticLab achieves stronger visual-language generalization without task-specific training.

#### F. Takeaways

Two lessons are most actionable. First, the end-to-end robustness of robotic agents like AgenticLab is bounded by the weakest module; in our setting, action checking is often the limiting factor, and strong task parsing cannot compensate for unreliable verification. Second, time budgets are binding in real-world deployment: dense verification improves robustness for long-horizon manipulation but can be expensive, whereas sparse verification reduces latency yet often degrades performance once errors accumulate.

For practitioners building similar manipulation agents, the key recommendation is to optimize for closed-loop consistency rather than richer open-loop reasoning. In practice, closing the loop can substantially improve manipulation performance, because well-designed verification enables timely detection of execution failures and triggers effective retrying and re-planning before the system drifts into harder-to-recover states. Finally, in our benchmark, the Gemini family is consistently strong across embodied modules, making it a practical backbone for real-world robot agent deployment, while smaller local models such as Qwen2.5-VL-7B and Molmo-7B remain competitive for visual grounding and can be useful building blocks for cost-effective compositional pipelines.

#### VII. LIMITATIONS AND FUTURE WORK

While AgenticLab serves as a practical testbed for evaluating closed-loop real-robot manipulation agents, it has several limitations:

1. Predefined symbolic domain. AgenticLab relies on manually authored PDDL domain files, which require expert effort to design. A promising future direction is to explore learning-based domain modeling, where VLMs or task-specific models generate, refine, and validate PDDL domains from task descriptions and executions, thereby enabling more scalable domain adaptation.

2. Predefined action primitives. AgenticLab currently relies on a set of hand-designed primitives. This can limit fine-grained behaviors and often requires additional engineering to support new skills. Future work can augment the primitive set with learning-based atomic skills while preserving the same agent interface.

3. Verification Latency. While frequent checks improve system reliability, they add significant overhead. To mitigate this, future work can explore distilling large VLMs into smaller, specialized models for efficient action verification, thereby optimizing the trade-off between speed and robustness.

## REFERENCES

[1] Josh Achiam, Steven Adler, Sandhini Agarwal, Lama Ahmad, Ilge Akkaya, Florencia Leoni Aleman, Diogo Almeida, Janko Altenschmidt, Sam Altman, Shyamal Anadkat, et al. Gpt-4 technical report. *arXiv preprint arXiv:2303.08774*, 2023.

[2] An-Chieh Cheng, Hongxu Yin, Yang Fu, Qiushan Guo, Ruihan Yang, Jan Kautz, Xiaolong Wang, and Sifei Liu. Spatialrgpt: Grounded spatial reasoning in vision-language models. *Advances in Neural Information Processing Systems*, 37:135062–135093, 2024.

[3] Hao-Tien Lewis Chiang, Zhusuo Xu, Zipeng Fu, Mithun George Jacob, Tingnan Zhang, Tsang-Wei Edward Lee, Wenhao Yu, Connor Schenck, David Rendleman, Dhruv Shah, et al. Mobility vla: Multimodal instruction navigation with long-context vlms and topological graphs. *arXiv preprint arXiv:2407.07775*, 2024.

[4] Jae-Woo Choi, Youngwoo Yoon, Hyobin Ong, Jaehong Kim, and Minsu Jang. Lota-bench: Benchmarking language-oriented task planners for embodied agents. *arXiv preprint arXiv:2402.08178*, 2024.

[5] Gheorghe Comanici, Eric Bieber, Mike Schaeckermann, Ice Pasupat, Noveen Sachdeva, Inderjit Dhillon, Marcel Blistein, Ori Ram, Dan Zhang, Evan Rosen, et al. Gemini 2.5: Pushing the frontier with advanced reasoning, multimodality, long context, and next generation agentic capabilities. *arXiv preprint arXiv:2507.06261*, 2025.

[6] Jiafei Duan, Wentao Yuan, Wilbert Pumacay, Yi Ru Wang, Kiana Ehsani, Dieter Fox, and Ranjay Krishna. Manipulate-anything: Automating real-world robots using vision-language models. *arXiv preprint arXiv:2406.18915*, 2024.

[7] Hao-Shu Fang, Minghao Gou, Chenxi Wang, and Cewu Lu. Robust grasping across diverse sensor qualities: The graspNet-1billion dataset. *The International Journal of Robotics Research*, 2023.

[8] Kuan Fang, Yuxin Chen, Xinghao Zhu, Farzad Niroui, Lingfeng Sun, and Jiuguang Wang. Saga: Open-world mobile manipulation via structured affordance grounding. *arXiv e-prints*, pages arXiv–2512, 2025.

[9] Senyu Fei, Siyin Wang, Junhao Shi, Zihao Dai, Jikun Cai, Pengfang Qian, Li Ji, Xinzhe He, Shiduo Zhang, Zhaoye Fei, et al. Libero-plus: In-depth robustness analysis of vision-language-action models. *arXiv preprint arXiv:2510.13626*, 2025.

[10] Malte Helmert. The fast downward planning system. *Journal of Artificial Intelligence Research*, 26:191–246, 2006.

[11] Edward J Hu, Yelong Shen, Phillip Wallis, Zeyuan Allen-Zhu, Yuanzhi Li, Shean Wang, Lu Wang, Weizhu Chen, et al. Lora: Low-rank adaptation of large language models. *ICLR*, 1(2):3, 2022.

[12] Wenlong Huang, Chen Wang, Ruohan Zhang, Yunzhu Li, Jiajun Wu, and Li Fei-Fei. Voxposer: Composable 3d value maps for robotic manipulation with language models. *arXiv preprint arXiv:2307.05973*, 2023.

[13] Wenlong Huang, Chen Wang, Yunzhu Li, Ruohan Zhang, and Li Fei-Fei. Rekep: Spatio-temporal reasoning of relational keypoint constraints for robotic manipulation. *arXiv preprint arXiv:2409.01652*, 2024.

[14] Physical Intelligence, Kevin Black, Noah Brown, James Darpinian, Karan Dhabalia, Danny Driess, Adnan Es-mail, Michael Equi, Chelsea Finn, Niccolò Fusai, et al. pi0.5: a vision-language-action model with open-world generalization. *arXiv preprint arXiv:2504.16054*, 2025.

[15] Mukul Khanna, Ram Ramrakhy, Gunjan Chhablani, Sriram Yenamandra, Theophile Gervet, Matthew Chang, Zsolt Kira, Devendra Singh Chaplot, Dhruv Batra, and Roozbeh Mottaghi. Goat-bench: A benchmark for multi-modal lifelong navigation. In *Proceedings of the IEEE/CVF Conference on Computer Vision and Pattern Recognition*, pages 16373–16383, 2024.

[16] Moo Jin Kim, Karl Pertsch, Siddharth Karamcheti, Ted Xiao, Ashwin Balakrishna, Suraj Nair, Rafael Rafailov, Ethan Foster, Grace Lam, Pannag Sanketi, et al. Openvla: An open-source vision-language-action model. *arXiv preprint arXiv:2406.09246*, 2024.

[17] Alexander Kirillov, Eric Mintun, Nikhila Ravi, Hanzi Mao, Chloe Rolland, Laura Gustafson, Tete Xiao, Spencer Whitehead, Alexander C Berg, Wan-Yen Lo, et al. Segment anything. In *Proceedings of the IEEE/CVF international conference on computer vision*, pages 4015–4026, 2023.

[18] Manling Li, Shiyu Zhao, Qineng Wang, Kangrui Wang, Yu Zhou, Sanjana Srivastava, Cem Gokmen, Tony Lee, Erran Li Li, Ruohan Zhang, et al. Embodied agent interface: Benchmarking llms for embodied decision making. *Advances in Neural Information Processing Systems*, 37:100428–100534, 2024.

[19] Bo Liu, Yuqian Jiang, Xiaohan Zhang, Qiang Liu, Shiqi Zhang, Joydeep Biswas, and Peter Stone. Llm+p: Empowering large language models with optimal planning proficiency. *arXiv preprint arXiv:2304.11477*, 2023.

[20] Fangchen Liu, Kuan Fang, Pieter Abbeel, and Sergey Levine. Moka: Open-world robotic manipulation through mark-based visual prompting. *arXiv preprint arXiv:2403.03174*, 2024.

[21] Peiqi Liu, Yaswanth Orru, Jay Vakil, Chris Paxton, Nur Muhammad Mahi Shafiqullah, and Lerrel Pinto. Ok-robot: What really matters in integrating open-knowledge models for robotics. *arXiv preprint arXiv:2401.12202*, 2024.

[22] Xiao Liu, Hao Yu, Hanchen Zhang, Yifan Xu, Xuanyu Lei, Hanyu Lai, Yu Gu, Hangliang Ding, Kaiwen Men, Kejuan Yang, et al. Agentbench: Evaluating llms as agents. *arXiv preprint arXiv:2308.03688*, 2023.

[23] Xiao Liu, Tianjie Zhang, Yu Gu, Iat Long Jong, Yifan Xu, Xixuan Song, Shudan Zhang, Hanyu Lai, Xinyi Liu, Hanlin Zhao, et al. Visualagentbench: Towards large multimodal models as visual foundation agents. *arXiv preprint arXiv:2408.06327*, 2024.

[24] Arjun Majumdar, Anurag Ajay, Xiaohan Zhang, Pranav Putta, Sriram Yenamandra, Mikael Henaff, Sneha Silwal, Paul Mcvay, Oleksandr Maksymets, Sergio Arnaud, et al. Openeqa: Embodied question answering in the era of foundation models. In *Proceedings of the IEEE/CVF conference on computer vision and pattern recognition*, pages 16488–16498, 2024.

[25] Luca Medeiros. Language segment-anything. <https://github.com/luca-medeiros/lang-segment-anything>, 2023.

[26] Shivan Patel, Xinch Chen Yin, Wenlong Huang, Shubham Garg, Hooshang Nayyeri, Li Fei-Fei, Svetlana Lazebnik, and Yunzhu Li. A real-to-sim-to-real approach to robotic manipulation with vlm-generated iterative keypoint rewards. *arXiv preprint arXiv:2502.08643*, 2025.

[27] Chan Hee Song, Valts Blukis, Jonathan Tremblay, Stephen Tyree, Yu Su, and Stan Birchfield. Robospatial: Teaching spatial understanding to 2d and 3d vision-language models for robotics. *CoRR*, 2024.

[28] Gemini Robotics Team, Saminda Abeyruwan, Joshua Ainslie, Jean-Baptiste Alayrac, Montserrat Gonzalez Arenas, Travis Armstrong, Ashwin Balakrishna, Robert Baruch, Maria Bauza, Michiel Blokzijl, et al. Gemini robotics: Bringing ai into the physical world. *arXiv preprint arXiv:2503.20020*, 2025.

[29] Georgios Tzias and Hamidreza Kasaei. Towards open-world grasping with large vision-language models. *arXiv preprint arXiv:2406.18722*, 2024.

[30] Jimmy Wu, Rika Antonova, Adam Kan, Marion Lepert, Andy Zeng, Shuran Song, Jeannette Bohg, Szymon Rusinkiewicz, and Thomas Funkhouser. Tidybot: Personalized robot assistance with large language models. *Autonomous Robots*, 47(8):1087–1102, 2023.

[31] An Yang, Anfeng Li, Baosong Yang, Beichen Zhang, Binyuan Hui, Bo Zheng, Bowen Yu, Chang Gao, Chengan Huang, Chenxu Lv, et al. Qwen3 technical report. *arXiv preprint arXiv:2505.09388*, 2025.

[32] Rui Yang, Hanyang Chen, Junyu Zhang, Mark Zhao, Cheng Qian, Kangrui Wang, Qineng Wang, Teja Venkat Koripella, Marziyeh Movahedi, Manling Li, et al. Embodiedbench: Comprehensive benchmarking multi-modal large language models for vision-driven embodied agents. *arXiv preprint arXiv:2502.09560*, 2025.

[33] Haoming Ye, Yunxiao Xiao, Cewu Lu, and Panpan Cai. Pretraining a unified pddl domain from real-world demonstrations for generalizable robot task planning. *arXiv preprint arXiv:2507.21545*, 2025.

[34] Xiaohan Zhang, Zainab Altawee, Yohei Hayamizu, Yan Ding, Saeid Amiri, Hao Yang, Andy Kaminski, Chad Esselink, and Shiqi Zhang. Dkprompt: Domain knowledge prompting vision-language models for open-world planning. *arXiv preprint arXiv:2406.17659*, 2024.

[35] Xiaohan Zhang, Yan Ding, Yohei Hayamizu, Zainab Altawee, Yifeng Zhu, Yuke Zhu, Peter Stone, Chris Paxton, and Shiqi Zhang. Llm-grop: Visually grounded robot task and motion planning with large language models. *The International Journal of Robotics Research*, 2025.

[36] Xueyang Zhou, Yangming Xu, Guiyao Tie, Yongchao Chen, Guowen Zhang, Duanfeng Chu, Pan Zhou, and Lichao Sun. Libero-pro: Towards robust and fair evaluation of vision-language-action models beyond memorization. *arXiv preprint arXiv:2510.03827*, 2025.

## APPENDIX A IMPLEMENTATION DETAILS

### A. Implementation Overview

We describe the AgenticLab pipeline in Algorithm 1. The system supports multiple action types, such as pick and place. We illustrate the main loop with pick; the remaining actions follow the same structure with minor, action-specific changes. For example, place performs only Detect and does not invoke AnyGrasp.

---

#### Algorithm 1 AgenticLab Pipeline

##### Require:

Vision-Language Model  $\mathcal{M}$   
 Task Instruction  $l$   
 PDDL Domain File  $D$   
 Text Prompt for Task Parser  $p_{\text{task}}$   
 Text Prompt for Action Checker  $p_{\text{checker}}$   
 Text Prompt for Grasp Planner  $p_{\text{grasp}}$   
 Text Prompt for Goal Checker  $p_{\text{goal}}$   
 Initial Observation  $s_0^{\text{sh}}$  // “sh” denotes shoulder camera.

```

// Query  $\mathcal{M}$  to parse the task into  $N$  actions  $\{a_k\}_{k=1}^N$ .
// Each action specifies preconditions, target object, and effects.
1:  $\{a_k\}_{k=1}^N = \mathcal{M}(p_{\text{task}}, l, D, s_0)$ 
2: for action  $\{a_k\}_{k=1}^N$  do
3:   Get observation  $s_k^{\text{sh}}$ 
      // Verify precondition.
4:   if not  $\mathcal{M}(p_{\text{checker}}, a_k^{\text{pre}}, s_k^{\text{sh}})$  then
5:     Go to step 1
6:   end if
      // Detect the target object.
7:    $\text{bbox}_k^{\text{sh}} = \text{Detect}(s_k^{\text{sh}}, a_k^{\text{target}})$ 
      // Generate the grasp pose.
8:    $\pi_k = \text{AnyGrasp}(s_k^{\text{sh}}, \text{bbox}_k^{\text{sh}}, a_k)$ 
      // Evaluate the generated grasp.
9:   if not  $\mathcal{M}(p_{\text{grasp}}, \pi_k, s_k^{\text{sh}})$  then
10:    Move end-effector to  $\pi_k$  to get wrist camera view
11:    Get observation  $s_k^{\text{wrist}}$  from wrist camera
12:     $\text{bbox}_k^{\text{wrist}} = \text{Detect}(s_k^{\text{wrist}}, a_k^{\text{target}})$ 
13:     $\pi_k = \text{AnyGrasp}(s_k^{\text{wrist}}, \text{bbox}_k^{\text{wrist}}, a_k)$ 
14:  end if
15:  Execute  $\pi_k$ 
16:  Get post-action observation  $s_k^{\text{post}}$ 
      // Verify effect.
17:  if not  $\mathcal{M}(p_{\text{checker}}, a_k^{\text{effect}}, s_k^{\text{post}})$  then
18:    Go to step 3
19:  end if
20: end for
      // Verify task completion.
21: if not  $\mathcal{M}(p_{\text{goal}}, s_N^{\text{post}})$  then
22:   Go to step 1
23: end if

```

---

### B. Qualitative Walkthrough and I/O Specifications

We utilize a unified interface for all VLM components. To ensure reproducibility, we provide a concrete walkthrough of the main modules.

**Task Parser.** To bridge natural-language instructions and symbolic planning, the task parser facilitates the translation from instruction to PDDL. As illustrated in Table III, it operates as follows:

- Input: The model receives the domain definition (Fig. 9), scene observation, and a user instruction (e.g., “stack the cubes...”).
- Reasoning: The VLM generates a PDDL problem file (Fig. 10) that defines the initial state and goal conditions based on the visual observation.
- Output: A classical planner, Fast Downward [10], solves this PDDL to produce an executable action sequence (Fig. 11).

**Action Checker.** To ensure closed-loop reasoning and robustness, the action checker validates both preconditions and effects. Table IV demonstrates this capability.

A detailed input example for the action checker is shown in Fig. 12, including representative precondition and effect queries for pick actions under the shoulder camera view. Figs. 13-16 further visualize corresponding JSON outputs from different VLMs, illustrating how the checker reports per-predicate satisfaction and diagnoses failure cases when evaluated effects are not correct.

**Grasp Planner.** Fig. 17 illustrates the input used to evaluate semantic correctness and physical feasibility: the proposed grasp pose visualized in the local point cloud. We provide ground-truth executability labels (a-e) for better understanding. The corresponding model reasoning and judgments are detailed in Figs. 18-22. The model evaluates whether the pose targets the correct semantic object and is collision-free. Crucially, a REJECT decision triggers the system to switch to the wrist camera for a close-up re-evaluation and re-planning.

## APPENDIX B EXPERIMENT DETAILS

### A. Task Progress Score

In both the compositional vs. single-VLM experiments and the ablation study, we measure performance using a task progress score derived from a structured action-sequence rubric. The score measures how much of the intended plan was completed, while penalizing unnecessary actions and final goal-check failures, making it more informative than binary success. This structured scoring system allows for consistent evaluation and comparison of task performance.

Concretely, let  $N$  be the total number of executed actions,  $N_{\text{done}}$  the number of actions that match the required action sequence, and  $N_{\text{extra}}$  the number of redundant actions. Denote  $p \in \{0, 1\}$  as a binary penalty for goal-checker error, where  $p = 1$  indicates that the goal checker failed to correctly assess

### PDDL Domain: stacking

```

(define (domain stacking)
  (:requirements :strips :typing)
  (:types cube cloth plate bowl mat paper - object
    purple-cube blue-cube orange-cube yellow-cube green-cube - cube)
  (:predicates
    (on-top-of ?o1 - object ?o2 - object)
    (hand-empty)
    (holding ?o - object)
    (clear ?o - object))

  (:action pick
    :parameters (?obj - object ?underobj - object)
    :precondition (and (hand-empty)
      (clear ?obj)
      (on-top-of ?obj ?underobj))
    :effect (and (holding ?obj)
      (clear ?underobj)
      (not (hand-empty))
      (not (on-top-of ?obj ?underobj))
      (not (clear ?obj)))))

  (:action place-on-object
    :parameters (?obj - object ?target - object)
    :precondition (and (holding ?obj)
      (clear ?target))
    :effect (and (on-top-of ?obj ?target)
      (hand-empty)
      (clear ?obj)
      (not (clear ?target))
      (not (holding ?obj)))))


```

Fig. 9: The defined PDDL domain of stacking task.

#### The input request contains:

- A string describing the multi-stage manipulation task.
- An image of the current table-top environment captured from a shoulder camera.
- A PDDL domain file defining available predicates and actions.
- An example problem in both natural language and PDDL format for few-shot learning.

#### The output response is a JSON object containing:

- **objects\_identified**: A list of objects identified from the scene. Each object has a name (PDDL identifier, e.g., “blue-block-1”), type (object category), and description (natural language description of the object).
- **reasoning**: A string providing brief analysis of task-relevant objects, their types, spatial relationships, and task requirements.
- **updated\_domain**: The complete PDDL domain file with new object types added if the task mentions types not in the original domain.
- **problem\_pddl**: A complete PDDL problem file containing the :objects section listing all identified objects, :init section describing the current state, and :goal section specifying the desired final state.

TABLE III: The high-level reasoning prompt for task parser. It analyzes the scene image and task instruction to generate a structured PDDL representation that can be solved by a classical planner.

the final task state. We define:

$$\text{Score} = \frac{N_{\text{done}} - N_{\text{extra}}}{N} - 0.1p.$$

The redundant-action penalty is important because VLMs sometimes introduce redundant goals when generating the problem PDDL, which can trigger unnecessary steps, this behavior is especially common in the crossword task.

#### B. Module Benchmark Details

**Data Annotation:** We report the data annotation details used in our module-level benchmark.

1. Action Checker. We collect action-checker evaluation data from real rollouts of the AgenticLab pipeline, resulting in 61 verification instances across 7 different scenes and 5 tasks. For each model, we run three trials and report the average success rate, latency, and token usage.

2. Grasp Planner. We curate 50 grasp-planning instances covering diverse objects. Executability is labeled from real-

**The input request contains:**

- A PDDL action to be executed (e.g., (pick apple-1)).
- The preconditions for the action in PDDL format (e.g., (and (hand-empty) (clear apple-1))).
- An image of the current scene captured from a shoulder camera showing the robot gripper and workspace.
- A reference guide explaining PDDL predicates such as hand-empty, holding, clear, on-table, and on-top-of.

**The output response is a JSON object containing:**

- **conditions\_analysis:** A list of individual condition evaluations. Each entry contains a condition (the exact predicate string), satisfied (boolean indicating if the condition holds), and observation (visual evidence from the image supporting the evaluation).
- **success:** A boolean indicating whether ALL preconditions are satisfied based on logical operators (and/or/not).
- **reasoning:** A string providing the overall conclusion explaining why the preconditions are or are not satisfied.
- **failed\_conditions:** A list of predicate strings that are NOT satisfied (empty if all conditions are met).

TABLE IV: The precondition verification prompt for action checker. It visually validates whether the current scene satisfies all preconditions before executing a planned action, enabling closed-loop error detection.

PDDL Problem: stacking	Action Sequence Solved by PDDL Planner
<pre> (define (problem stacking-stack-cubes-on-pink-   plate)   (:domain vlmrobobench)    (:objects     green-cube-1 - green-cube     yellow-cube-1 - yellow-cube     orange-cube-1 - orange-cube     blue-cube-1 - blue-cube     pink-plate-1 - pink-plate     turquoise-plate-1 - turquoise-plate     cream-plate-1 - cream-plate   )    (:init     (hand-empty)     (on-top-of yellow-cube-1 blue-cube-1)     (on-top-of blue-cube-1 cream-plate-1)     (on-top-of green-cube-1 orange-cube-1)     (on-top-of orange-cube-1 turquoise-plate-1)     (clear yellow-cube-1)     (clear green-cube-1)     (clear pink-plate-1)   )    (:goal     (and       (on-top-of green-cube-1 pink-plate-1)       (on-top-of yellow-cube-1 green-cube-1)       (on-top-of orange-cube-1 yellow-cube-1)       (on-top-of blue-cube-1 orange-cube-1)     )   ) ) </pre>	<pre> (pick green-cube-1 orange-cube-1); (place-on-object green-cube-1 yellow-cube-1); (pick orange-cube-1 blue-plate-1); (place-on-object orange-cube-1 pink-plate-1); (pick green-cube-1 yellow-cube-1); (place-on-object green-cube-1 blue-plate-1); (pick yellow-cube-1 blue-cube-1); (place-on-object yellow-cube-1 green-cube-1); (pick blue-cube-1 white-plate-1); (place-on-object blue-cube-1 orange-cube-1); (pick yellow-cube-1 green-cube-1); (place-on-object yellow-cube-1 blue-cube-1); (pick green-cube-1 blue-plate-1); (place-on-object green-cube-1 yellow-cube-1) </pre>

Fig. 10: The PDDL Problem File Generated by Gemini 3 Flash. Stack the cubes on the pink plate from bottom to top: Orange Blue Yellow and Green cubes

world outcomes, where a grasp is considered valid if it picks the correct object and executes without collisions. Each model is evaluated over three runs. Notably, local models frequently collapse to near-constant true/false outputs, indicating limited capability as grasp planners under this protocol.

3. Object Detector. We collect 21 real-world camera inputs and annotate object regions using SAM masks [17] and corresponding bounding boxes. We compute (i) point-in-mask success rate, based on whether the VLM-predicted point lies

Fig. 11: Action sequence obtained by solving the updated domain file with the generated problem file.

inside the SAM mask, and (ii) bounding-box IoU, defined as the overlap area divided by the union area between the predicted box and the annotated box. Each model is tested three times and we report averaged results.

4. Goal Checker. For task-level parsing evaluation, we record 16 final-scene cases and ask the VLM to judge whether the task goal is satisfied. Each model is evaluated with three runs. Ground-truth labels are provided by five human annotators, who determine success based on the goal specification and the task prompt.

**Module Benchmark Results:** We summarize per-module performance with a radar chart in Fig. 23. Each axis corresponds to a module-level metric, and we normalize all scores to  $[0, 1]$  so that larger values indicate better performance. We also report efficiency across VLM backends using the average latency in Fig. 24 and token usage in Fig. 25, both aggregated over the same module benchmark runs.

**Human Evaluation Interface:** Evaluating the task parser in open-world scenes benefits from a human study, since fully automatic evaluation can rely on brittle, hand-crafted heuristics. We therefore conduct a human study and build a lightweight labeling UI that supports efficient, reproducible evaluation while ensuring fair, blinded comparison across models.

As shown in Fig. 26, participants are shown only (i) the task



(a) Precondition check (pick can-1)

(b) Effect check (pick can-1)

(c) Effect check (pick oreo-pack-1)

Fig. 12: Precondition/effect checks for pick actions across objects.

### Gpt-5.2 Precondition Check Result: pick can-1

```
{
  "success": true,
  "reasoning": "Both preconditions (hand-empty) and (on-table can-1) are satisfied. The robot gripper is empty and ready to pick, and the can is resting on the table as required. Since the action uses an AND operator, all conditions must be met, and they are.",
  "elapsed_time": 11.282440900802612,
  "detailed_analysis": [
    {
      "condition": "(hand-empty)",
      "satisfied": true,
      "observation": "The robot gripper is visible in the upper right corner and is not holding any object; it is open and positioned above the table, indicating it is empty."
    },
    {
      "condition": "(on-table can-1)",
      "satisfied": true,
      "observation": "The cylindrical can (can-1) is clearly placed directly on the white table surface, with no other objects on top of it or between it and the table."
    }
  ]
}
```

Fig. 13: Precondition check for picking can (success, GPT-5.2).

goal, (ii) the initial scene image at the start of the episode, and (iii) the action sequence produced by the task parser. The model identity is hidden. Participants judge whether the provided action sequence can reasonably achieve the goal under the given initial scene conditions.

We evaluate four task categories: sorting, stacking, crossword, and kitchen. We recruited five participants and collected 468 action-sequence judgments in total. To improve reliability, we perform three full passes over the complete set and report results aggregated across rounds.

Table V lists the natural language instructions used in our task parser benchmark, covering the four evaluation categories described above.

#### C. Ablation Experiment Protocol

For the action-checker ablation, we evaluate performance using the task progress score in Appendix B-A and measure

efficiency by runtime under controlled human disturbances. We compare three action-checker configurations: no action checker, a goal checker only, and the full action checker. The goal-checker-only configuration performs a single verification at the end of execution, such as checking whether the final goal is satisfied after all planned actions complete. In contrast, the full action checker verifies outcomes step by step after each action.

We use the following disturbance protocols.

1. No disturbance, sorting. We execute the sorting task without human intervention, placing food items into the box and toys into the bowl.
2. One disturbance, sorting. During the first pick, we move the target object to induce a misgrasp and simulate grasp failure.
3. Two disturbances, sorting. In addition to the first-pick disturbance, we move the target placement location during the

### Gpt-5.2 Effect Check Result: pick can-1

```
{
  "success": false,
  "reasoning": "All three expected effects must be achieved for success. However, none of them are satisfied: the robot is not holding any object, the hand is empty (contradicting 'not (hand-empty)'), and no object has been lifted off the table. Thus, the action '(pick oreo-pack-1)' was not successfully executed.",
  "elapsed_time": 14.711339473724365,
  "failed_conditions": [
    "(holding ?x)",
    "(not (hand-empty))",
    "(not (on-table ?x))"
  ],
  "detailed_analysis": [
    {
      "effect": "(holding ?x)",
      "achieved": false,
      "observation": "The robot gripper is not holding any object. The gripper is open and empty, with no visible item grasped."
    },
    {
      "effect": "(not (hand-empty))",
      "achieved": false,
      "observation": "The gripper is empty, so the condition '(not (hand-empty))' is false. The hand is indeed empty."
    },
    {
      "effect": "(not (on-table ?x))",
      "achieved": false,
      "observation": "Since no object is being held, there is no '?x' that has been removed from the table. Therefore, this condition cannot be satisfied as no object has been picked up."
    }
  ]
}
```

Fig. 14: Effect check for picking can (fail, GPT-5.2).

final place action to simulate misplacement under a shifted goal configuration.

4. One disturbance, stacking. To test a sequential task where later outcomes depend on earlier actions, we move the target block during the first grasp to induce a disturbance.

#### D. VLA Fine-tuning Setup

We fine-tune the pretrained  $\pi_{0.5}$  VLA policy [14] on two tabletop manipulation tasks: sorting and stacking. Training configurations are provided in Table VI.

For sorting, we collect 40 human demonstrations, evenly split into two instruction variants: 20 episodes of “Grab the food to the bowl” and 20 episodes of “Grab the toys to the bin”. For stacking, we collected 30 demonstrations consisting of 10 episodes for each of three stacking orders: green-yellow-orange, yellow-green-orange, and orange-yellow-green.

We initialize the policy from the  $\pi_{0.5}$ -base checkpoint. To retain pretrained visual representations, we freeze the vision encoder and fine-tune only the reasoning and action components via Low-Rank Adaptation (LoRA) [11]. Specifically, we

apply LoRA to the linear projection layers in the Attention and FFN modules for both the VLM backbone and the flow-matching action expert. For all methods, we use the same perception setup consisting of one global camera and one wrist camera to ensure a fair comparison.

Qwen-VL-Plus Effect Check Result: pick can-1

```
{
  "success": false,
  "reasoning": "The action 'pick can-1' was executed, but there is no visible can-1 in the scene. The table contains a banana, a tennis ball, and two empty containers (blue and white), but no can. Therefore, none of the expected effects -- (holding ?x), (not (hand-empty)), or (not (on-table ?x)) -- can be verified as achieved because the target object 'can-1' does not appear to exist or be present in the environment.",
  "elapsed_time": 16.5667142868042,
  "failed_conditions": [
    "(holding ?x)",
    "(not (hand-empty))",
    "(not (on-table ?x))"
  ]
}
```

Fig. 15: Effect check for picking can (fail, Qwen-VL-Plus).

Task	Language Description
Sort	Sort the fruits into the white bin and all other objects into the blue bin.
Stack (3 cubes)	Stack the cubes on the pink plate from bottom to top: Green, Orange, and Blue.
Stack (4 cubes)	Stack the cubes on the pink plate from bottom to top: Green, Yellow, Orange, and Blue.
Crossword	Fill the numbered slots using the provided blocks to solve the crossword puzzle. You do not need to use all blocks or all slots.
Kitchen A	Put the spice bottle into the top drawer and close it.
Kitchen B	Place the blue snack pack in the top drawer, then move the spice bottle from the drawer to the table, and finally close the drawer.
Kitchen C	A chicken leg is in the pot. Take out the chicken leg, place it in the bowl, then put the spice bottle back into the top drawer and close the drawer.

TABLE V: Task list and language descriptions.

TABLE VI: VLA fine-tuning configuration. We apply LoRA to attention and FFN blocks for both the VLM backbone and the flow-matching action expert.

Component	Setting
Initialization	$\pi_{0.5}$ -Base
<b>VLM Backbone</b>	Gemma-2B
Vision Encoder	Frozen
LoRA Target	Attention & FFN Linear Projections
LoRA ( $r, \alpha$ )	(16, 16)
<b>Action Expert</b>	Gemma-300M
LoRA Target	Attention & FFN Linear Projections
LoRA ( $r, \alpha$ )	(32, 32)
Training Steps	10,000
Batch Size	64
Hardware	1 $\times$ NVIDIA A6000 (48 GB)
Training Duration	$\sim$ 38 Hours

### Gpt-5.2 Effect Check Result: pick oreo-pack-1

```
{
  "success": false,
  "reasoning": "All three expected effects must be achieved for success. However, none of them are satisfied: the robot is not holding any object, the hand is empty (contradicting 'not (hand-empty)'), and no object has been lifted off the table. Thus, the action '(pick oreo-pack-1)' was not successfully executed.",
  "elapsed_time": 14.711339473724365,
  "failed_conditions": [
    "(holding ?x)",
    "(not (hand-empty))",
    "(not (on-table ?x))"
  ],
  "detailed_analysis": [
    {
      "effect": "(holding ?x)",
      "achieved": false,
      "observation": "The robot gripper is not holding any object. The gripper is open and empty, with no visible item grasped."
    },
    {
      "effect": "(not (hand-empty))",
      "achieved": false,
      "observation": "The gripper is empty, so the condition '(not (hand-empty))' is false. The hand is indeed empty."
    },
    {
      "effect": "(not (on-table ?x))",
      "achieved": false,
      "observation": "Since no object is being held, there is no '?x' that has been removed from the table. Therefore, this condition cannot be satisfied as no object has been picked up."
    }
  ]
}
```

Fig. 16: Effect check for picking oreo pack (fail, GPT-5.2).

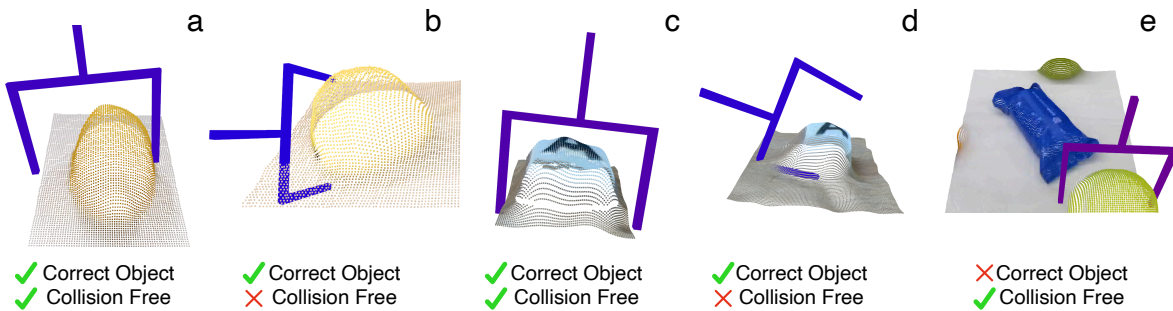


Fig. 17: Evaluation of proposed grasp poses. Ground-truth labels are provided below each example.

### Gemini 3 Flash Grasp Planning Result: pick lemon-1

```

"evaluation": {
    "action": "EXECUTE_GRASP",
    "object_correctness": {
        "is_correct_object": true,
        "confidence": 0.98,
        "reasoning": "The gripper frame is accurately centered over the yellow
                     point cloud representing the lemon. The fingers are wide enough to
                     enclose the object's bulk."
    },
    "collision_check": {
        "overlaps_with_surface": false,
        "confidence": 0.92,
        "reasoning": "The gripper fingers terminate above the table surface.
                     While the right finger is close to the table plane, there is no
                     evidence of deep penetration that would cause a failure."
    },
    "overall_reasoning": "The grasp is correctly targeted at the lemon and
                         maintains a safe distance from the table surface. It is a functional
                         grasp pose for the specified task.",
    "confidence": 0.95,
    "rejection_reason": null,
    "elapsed_time": 5.428056955337524
}

```

Fig. 18: Gemini 3 Flash output for example a in Fig. 17, planning the pick lemon-1 action.

### Gemini 3 Flash Grasp Planning Result: pick lemon-1

```

"evaluation": {
    "action": "REJECT_GRASP",
    "object_correctness": {
        "is_correct_object": true,
        "confidence": 0.95,
        "reasoning": "The gripper is correctly positioned around the yellow point
                     cloud cluster, which represents the 'lemon_collision' target object."
    },
    "collision_check": {
        "overlaps_with_surface": true,
        "confidence": 0.98,
        "reasoning": "The bottom finger of the gripper and a significant portion of
                     the gripper bridge (the vertical bar) are clearly submerged beneath
                     the table surface points (the tan point cloud). Visible surface points
                     are rendered on top of the gripper's blue geometry, indicating that
                     more than half of the lower finger is deeply intersecting with the
                     table plane."
    },
    "overall_reasoning": "Although the gripper is correctly targeting the lemon,
                         the grasp pose is physically impossible as the lower finger and part of the
                         gripper's base are positioned below the level of the table surface. This
                         deep penetration into the solid table surface would likely cause a hardware
                         failure or damage the robot.",
    "confidence": 0.98,
    "rejection_reason": "Severe collision with the table surface; the lower gripper
                         finger is almost entirely embedded in the table plane.",
    "elapsed_time": 20.040879011154175
}

```

Fig. 19: Gemini 3 Flash output for example b in Fig. 17, planning the pick lemon-1 action.

### Gemini 3 Flash Grasp Planning Result: pick block-a-1

```
"evaluation": {
    "action": "EXECUTE_GRASP",
    "object_correctness": {
        "is_correct_object": true,
        "confidence": 0.98,
        "reasoning": "The gripper frames the central mass of the point cloud, which represents the target block. It is well-centered and encompasses the bulk of the object."
    },
    "collision_check": {
        "overlaps_with_surface": false,
        "confidence": 0.9,
        "reasoning": "The gripper fingers are positioned on the sides of the object. While the tips reach towards the bottom of the point cloud, there is no evidence of deep penetration into the table surface that would constitute a catastrophic collision."
    },
    "overall_reasoning": "The grasp pose is correctly targeted at the specified object and appears to be collision-free relative to the visible point cloud data. The alignment is suitable for a successful pick operation.",
    "confidence": 0.95,
    "rejection_reason": null,
    "elapsed_time": 5.686762571334839
}
```

Fig. 20: Gemini 3 Flash output for example c in Fig. 17, planning the pick block-a-1 action.

### Gpt-5.2 Grasp Planning Result: pick block-a-1

```
"evaluation": {
    "action": "REJECT_GRASP",
    "object_correctness": {
        "is_correct_object": false,
        "confidence": 0.74,
        "reasoning": "The grasp frame (blue/purple pose indicator) is positioned primarily over the table/ground point cloud and appears offset to the side/below the main bulk of the target point cluster. The densest, raised object mass (block_a) is not centered within the implied gripper workspace; instead, the pose sits near a low-lying region, suggesting it would close on background/table points rather than the object."
    },
    "collision_check": {
        "overlaps_with_surface": false,
        "confidence": 0.62,
        "reasoning": "While the pose is close to the table surface, the visualization does not show a clear deep penetration of more than half a finger length into a solid plane; it looks like it would at most graze the fuzzy surface points. The primary failure is mis-targeting rather than a catastrophic collision."
    },
    "overall_reasoning": "The grasp pose is not aligned with or centered on the main elevated cluster corresponding to block_a, so it would likely miss the object and/or clamp on table/background points. No clearly destructive table intersection is evident, but object correctness is insufficient to execute.",
    "confidence": 0.71,
    "rejection_reason": "Grasp pose is not targeting the main body of block_a; it is offset toward the table/background rather than framing the object.",
    "elapsed_time": 7.609699964523315
}
```

Fig. 21: GPT-5.2 output for example d in Fig. 17, planning the pick block-a-1 action.

### Gemini 3 Pro Grasp Planning Result: pick blue-snack-pack-1

```
"evaluation": {
    "action": "REJECT_GRASP",
    "object_correctness": {
        "is_correct_object": false,
        "confidence": 1.0,
        "reasoning": "The grasp pose is positioned significantly offset to the
                     right of the target 'blue_snack_pack'. The gripper fingers frame the
                     white table surface and empty space next to the object, failing to
                     enclose the bulk or center of the blue snack pack."
    },
    "collision_check": {
        "overlaps_with_surface": false,
        "confidence": 0.9,
        "reasoning": "While the gripper is positioned low near the table plane,
                     there is no clear evidence of deep, destructive intersection with a
                     solid obstacle. The primary failure is spatial targeting."
    },
    "overall_reasoning": "The grasp is completely invalid because it misses the
                          target object. The gripper's closing region is located over the table
                          surface to the side of the snack pack, rather than around the object itself
                          .",
    "confidence": 1.0,
    "rejection_reason": "Gripper is completely missing the target object",
    "token_usage": 3771,
    "elapsed_time": 22.42589521408081
}
```

Fig. 22: Gemini 3 Pro output for example e in Fig. 17, planning the pick blue-snack-pack-1 action.

## Sub-module Performance Comparison across VLMs

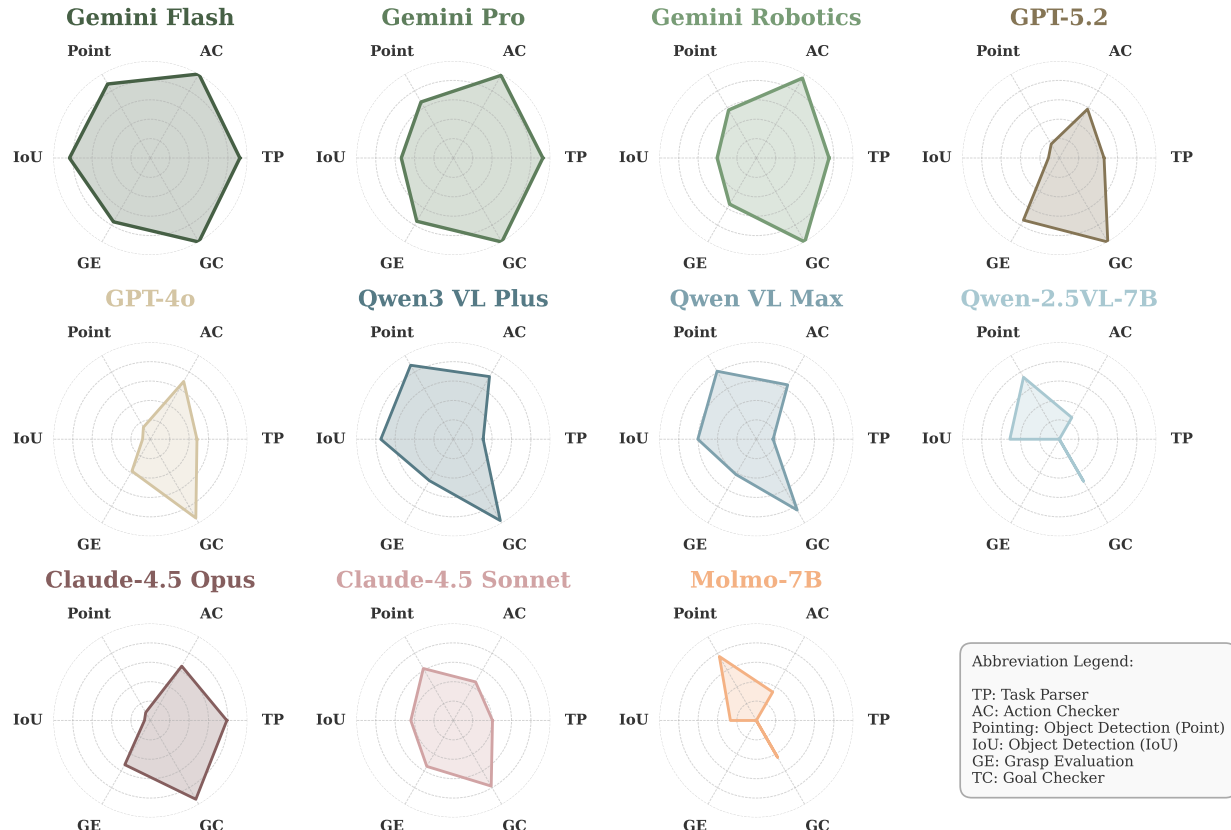


Fig. 23: Modular benchmark radar chart. Normalized per-module performance across the pipeline (higher is better). Each axis reports the corresponding module score.

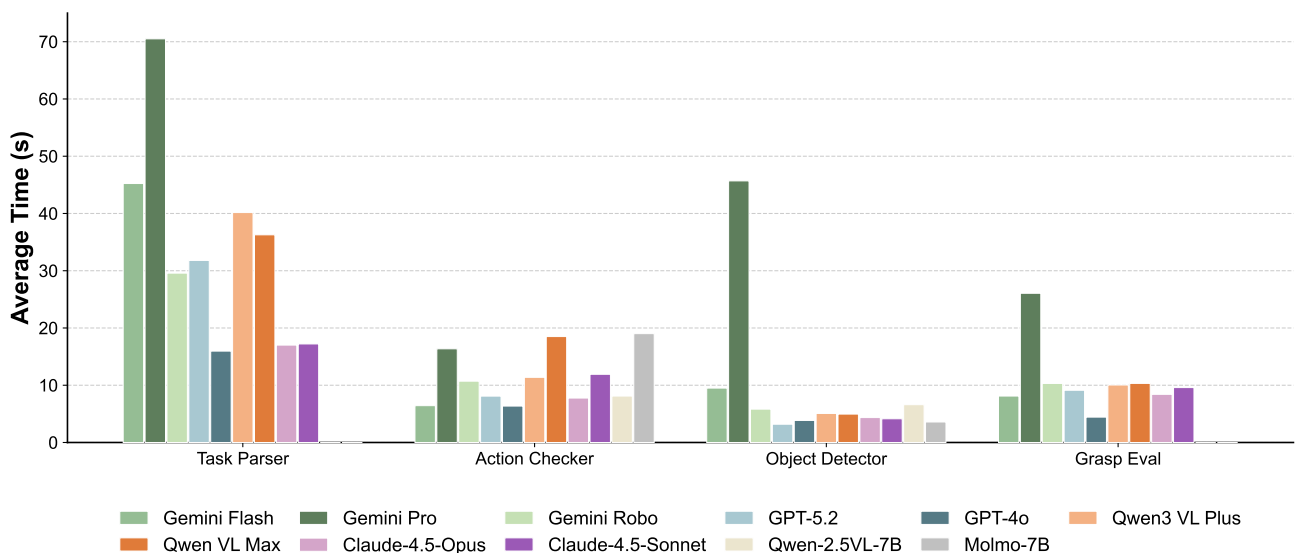


Fig. 24: Latency comparison across VLMs. Average runtime per module benchmark query.

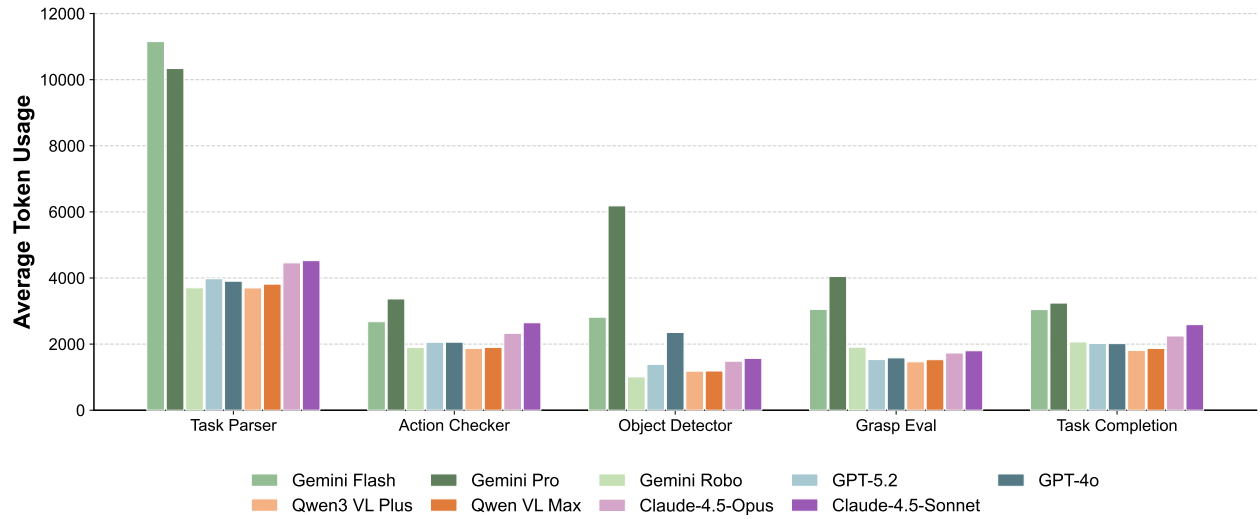


Fig. 25: Token usage comparison across VLMs. Average token consumption per module benchmark query.

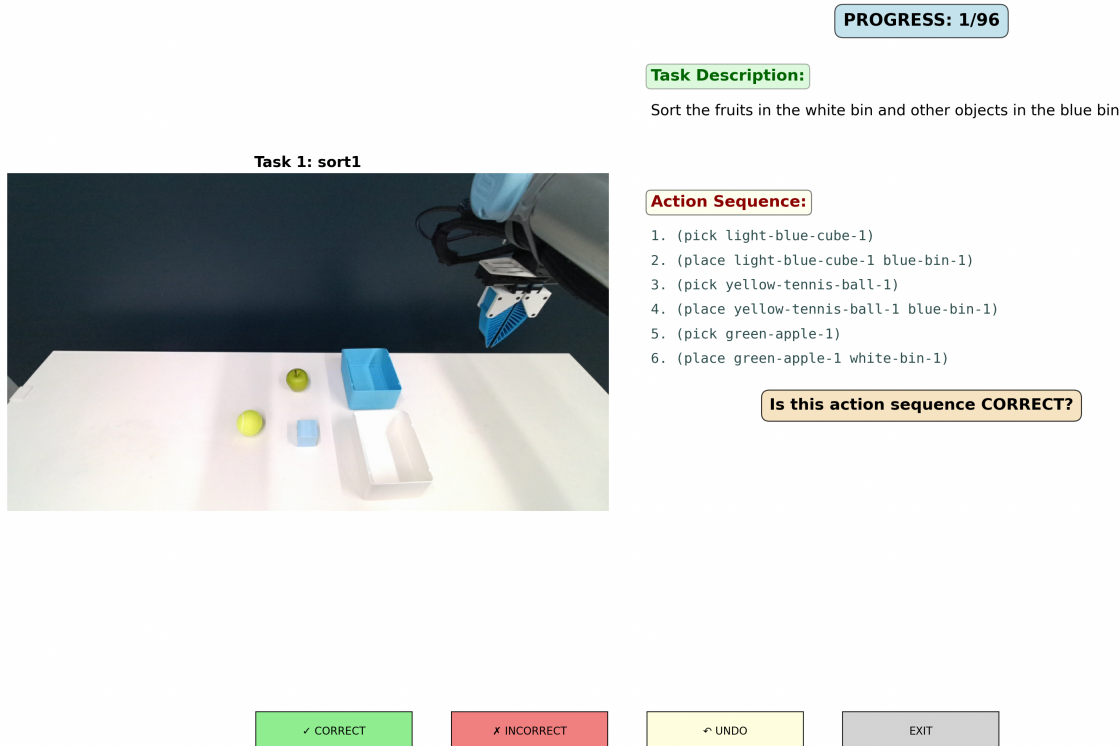


Fig. 26: Human evaluation UI.